Marine Pollution Bulletin 178 (2022) 113638

Contents lists available at ScienceDirect

Marine Pollution Bulletin

journal homepage: www.elsevier.com/locate/marpolbul

Reconstruction of the main phytoplankton population off the Changjiang Estuary in the East China Sea and its assemblage shift in recent decades: From observations to simulation

Fu-Tao Fang [a], Zhuo-Yi Zhu [a,b,*], Jian-Zhong Ge [a], Bing Deng [a], Jin-Zhou Du [a], Jing Zhang [a,b]

[a] State Key Laboratory of Estuarine and Coastal Research, East China Normal University, Shanghai 200241, China
[b] School of Oceanography, Shanghai Jiao Tong University, Shanghai 200030, China

ARTICLE INFO

Keywords:
Phytoplankton pigment
Sediment core
N/P ratio
SST
Diatoms-dinoflagellates shift
East China Sea

ABSTRACT

Under eutrophication background, the increasing dinoflagellates blooms relative to diatoms blooms off the Changjiang Estuary has caused much concern. We have provided sediment evidence for the first time that the time window of diatoms-to-dinoflagellates shift off the Changjiang Estuary in the East China Sea is early 1990s. Investigations to the water column revealed different surface-bottom concentration matchup patterns between peridinin (dinoflagellates) and fucoxanthin (diatoms), which suggests that the diatoms-dinoflagellates shift recorded in the sediment may have come from more dinoflagellate blooms since 1990s. Physical-biogeochemical 3D numerical simulations for the past decades suggest that the effect of increasing spring sea surface temperature and increasing N/P ratio on the diatoms-dinoflagellates shift is dominant and recessive, respectively.

1. Introduction

Understanding the phytoplankton assemblage in large river-affected marginal seas is essential in ecosystem and carbon cycle studies (Anderson et al., 2002). The Changjiang (Yangtze) River is one of the largest rivers in the world (Milliman and Meade, 1983), with the adjacent East China Sea (ECS) being one of the broadest continental shelves. A comprehensive understanding of the phytoplankton assemblage history off the Changjiang Estuary is essential in the assessment of ECS ecosystem and carbon cycling response to both anthropogenic activities and natural impacts (Jiang et al., 2014).

Off the Changjiang Estuary, the first bloom usually occurs in April, with occasional subsequent blooms throughout spring, summer, and early autumn (Li et al., 2014; Tang et al., 2006). Among the 12 months in every year, half of the blooms occurred in May (Li et al., 2014; Liu et al., 2013; Tang et al., 2006; Xiao et al., 2019). Diatoms (e.g., *Skeletonema costatum*) are the dominant groups throughout spring to autumn, whereas dinoflagellates (e.g., *Prorocentrum donghaiense* but sometimes ichthyotoxic dinoflagellate species) are becoming more and more common in spring (Liu et al., 2013; Liu et al., 2016; Zhou et al., 2017b). Other algae, such as cyanobacteria, haptophytes, and chrysophytes play a minor role off the Changjiang Estuary (Jiang et al., 2015; Liu et al., 2016; Mo et al., 2020). In viewing historical data, the increase in dinoflagellate blooms over diatom blooms in spring is repeatedly suggested (Li et al., 2014; Liu et al., 2013; Liu et al., 2016; Tang et al., 2006).

The potential cause of dinoflagellates-diatoms shift are suggested. First, the response of dinoflagellate growth to temperature is different from that of diatoms (Feng et al., 2021; Xiao et al., 2018). It is hence expected that under warming background, the growth of dinoflagellates would be promoted relative to diatoms. Indeed, pooled long term observations in the East China Sea suggests that the increasing spring dinoflagellates blooms is highly consistent with increasing sea surface temperature (SST) increase (Jiang et al., 2014; Liu et al., 2016; Xiao et al., 2018). The second frequently suggested cause is changes in riverine nutrient stoichiometry, namely extremely high riverine N/P ratio and deficiency in P (eutrophication) (Li et al., 2014; Ou et al., 2008; Wang et al., 2012; Xiao et al., 2018; Zhou et al., 2008; Zhou et al., 2019). Physiologically, *Prorocentrum donghaiense* (dinoflagellate) shows a better adaptability to P deficiency relative to diatoms (Ou et al., 2014; Ou et al., 2008). Further, the production of autoinhibitory produced by *Skeletonema costatum* (diatom) under P deficiency cannot affect *Prorocentrum donghaiense* growth (Wang et al., 2012). Additionally, other mentioned causes include alleviation in light (turbidity) (Zhou et al., 2017a), and water column stability (Jiang et al., 2019).

In spite of the discussion of mechanisms for such dinoflagellates-

* Corresponding author at: State Key Laboratory of Estuarine and Coastal Research, East China Normal University, Shanghai 200241, China
E-mail address: zhu.zhuoyi@sjtu.edu.cn (Z.-Y. Zhu).

https://doi.org/10.1016/j.marpolbul.2022.113638
Received 24 December 2021; Received in revised form 30 March 2022; Accepted 1 April 2022
Available online 9 April 2022

diatoms shift, when the diatoms-dinoflagellates shift started is not clear, which in turn affects our understanding of the mechanism. The suggested time windows covers a range of time, ranging from the 1980s (Jiang et al., 2014; Wang et al., 2018), 1990s (Ou et al., 2014), and 2000s (Li et al., 2014; Tang et al., 2006). Though the historical data is statistically processed to overcome the unbalance in data density of different decades (Tang et al., 2006), the possible reasons for an unclear history include bias in different sampling strategies during field observations (e.g., water vs. net) and potential missed blooms in historical data records due to limited cruises.

Preserved biomarkers in sediment provide another way to reconstruct historical phytoplankton assemblages. Due to the selective distribution of phytoplankton taxa, phytoplankton pigments in sediment cores are used to reconstruct phytoplankton assemblages. For two cores off the Changjiang Estuary, Li et al. (2011) found that both peridinin (key pigment for dinoflagellates) and fucoxanthin (key pigment for diatoms) increased since the early 1980s. The ratio of peridinin/fucoxanthin was later quantitatively checked in another core, indicating an increase in dinoflagellates relative to diatoms after 1995 (Zhu et al., 2014). Additional core along the Zhejiang coast in the ECS indicates variation of dinoflagellates and diatoms since 1960s till 2011 (Abate et al., 2017), but their cores were collected south of the Changjiang Estuary.

Although the overall phytoplankton biomass history (via Chla and degradations) and individual pigment patterns in the core are well documented (Abate et al., 2017; Kang et al., 2016; Li et al., 2011), the early diagenesis effect and stability difference among each pigment are seldom considered or distinguished when reconstructing historical phytoplankton assemblages in the Changjiang Estuary. Pigments are labile compounds with a range of stability during the early diagenesis process, and peridinin is more labile and unstable during the early diagenesis process than fucoxanthin (Reuss, 2005). Hence, changes in the sedimentary peridinin/fucoxanthin ratio are a combination of both real phytoplankton assemblage shifts throughout history and the early diagenesis effect (Zhu et al., 2014). For long time scale reconstruction (e.g., over thousands of years), this stability difference may play a minor role, but for the first tens of years, such an effect would be significant (Berner, 1980).

Furthermore, it is well known that various phytoplankton have their own vertical migration strategy. Dinoflagellates are known as swimmers, whereas diatoms achieve their vertical migration by modifying buoyancy (Sarthou et al., 2005; Smayda, 1997; Smayda, 2010). In addition, it has been reported that the sinking rate of *Prorocentrum donghaiense* at bloom sites is >10 times that at nonbloom sites in the ECS due to aggregate formation (Qiu et al., 2018). Given the complicated phytoplankton vertical migration status, it is necessary to compare and interpret the sediment core pigments with essential knowledge from the corresponding water column. To the best of our knowledge, such sedimentary core studies for pigments are still lacking.

Under this background, the scientific questions in this work are 1) what are the early diagenesis effects for various phytoplankton pigments in the core off the Changjiang Estuary and accordingly what is the time window for the diatoms-dinoflagellates shift as recorded by sediment and 2) with essential knowledge from the water column, what is the implication of the changes in the sedimentary peridinin/fucoxanthin ratio and what is the potential roles that SST increase and riverine P deficiency is playing in such assemblage shift? To address these questions, three approaches were used: (1) field observations to reveal key phytoplankton pigment concentrations couplings between surface and near-bottom waters in the water column among productive seasons; (2) a sedimentary pigment study to reconstruct the history and reveal the diatoms-dinoflagellates shift time-point; and (3) three-dimensional (3D) numerical modeling to investigate the correspondence between SST and phytoplankton change, as well as the potential roles of riverine nutrients. First, the surface–bottom coupling of peridinin (dinoflagellates), fucoxanthin (diatoms), and other key diagnostic pigments in the water column are compared. For the sedimentary pigments, an organic matter decay model is used to remove the early diagenesis effect for individual pigments. Then, the history of diatom proportions over selected key phytoplankton and diatoms-dinoflagellates shift time points were reconstructed. Finally, the 3D model was used to investigate the possible mechanism (or reason) of phytoplankton change history.

2. Materials and methods

2.1. Field sampling

Water samples and the sediment core were collected in different cruises. For water samples, three cruises were conducted in June, August, and October of 2006 (R/V *Beidou*), with sampling stations shown in Fig. 1b. The water depth of the whole study area is 15–97 m, with most stations having depths of 20–50 m (Fig. 1b). The temperature and salinity profiles were detected by a CTD (SEB 25), and surface and near-bottom waters were collected via precleaned Niskin samplers. Seawater samples were filtered immediately onboard using glass-fiber filters (precombusted Whatman GF/F) under mild vacuum in dim light. Filters were stored at −20 °C until analysis (Reuss and Conley, 2005).

Another cruise was conducted for the sediment core collection in July 2016 (R/V *Run Jiang*). Three cores (A5-4, A5-6, A6-5) were collected in the vicinity of the Changjiang Estuary. Immediately after collection, the cores were sectioned at 1 cm intervals using a clean stainless-steel knife, respectively, and samples were stored at −20 °C until analysis. The collection included a gravity corer collected at station A5-4 (122.83°E, 31.00°N; water depth 30 m; Fig. 1b).

2.2. Laboratory analyses

The analysis of phytoplankton pigments by high-performance liquid chromatography (HPLC; Agilent 1100; Agilent Technologies, USA) followed the method of Zapata et al. (2000) with slight modifications for filter samples (Zhu et al., 2009) and sediment samples (Zhu et al., 2014). Briefly, filters were ultrasonically extracted with dimethylformamide (DMF) in an ice-water bath. After centrifugation, the supernatant was filtered using a nylon filter (0.45 μm), and Milli-Q water (5:1 v/v) was added to avoid deformation of the early elution peak (Zapata and Garrido, 1991). The HPLC instrument was equipped with an online vacuum degasser, quaternary pump, autosampler, thermostatically controlled column, and diode-array detector. All procedures were performed under dim light, and extracts were stored at −80 °C prior to injection. The analytical column was a ZORBAX Eclipse XBD-C8 (Agilent Technologies) analytical 4.6 × 150 mm, 5 μm column. The mobile phase and elution gradient have been described previously (Zhu et al., 2009). Sediment samples were thawed at 4 °C and ultrasonically extracted twice with DMF. The extracts were combined, centrifuged, filtered, and injected as per filter samples. The extracted sediment was dried and weighed to obtain the dry weight. The initial mobile phase proportion in the sediment method was slightly different from the method for particles (Zhu et al., 2009; Zhu et al., 2014), in order to promote the separation of pigment peaks. Also, the elution time for preserved sedimentary pigments was longer (65 min) than that for particle samples (47 min).

Up to 19 pigments were identified, with their most common corresponding phytoplankton groups shown in Table S1. Pigments were identified on the basis of chromatographic retention times, as well as their spectrum scanned by the diode-array detector. Chla and Chlb (Sigma-Aldrich, USA) and the other pigments (DHI, Denmark) were used as standards. All peaks were manually integrated. A typical chromatogram for preserved sedimentary pigments is shown in supplemental materials (Fig. S2). The recoveries from filter and sediment samples were 95%–105% and 84%–101%, respectively. A pigment recovery experiment is described in the Supplemental Materials.

The sediment cores were dated by the excess ^{210}Pb ($^{210}Pb_{ex}$) and

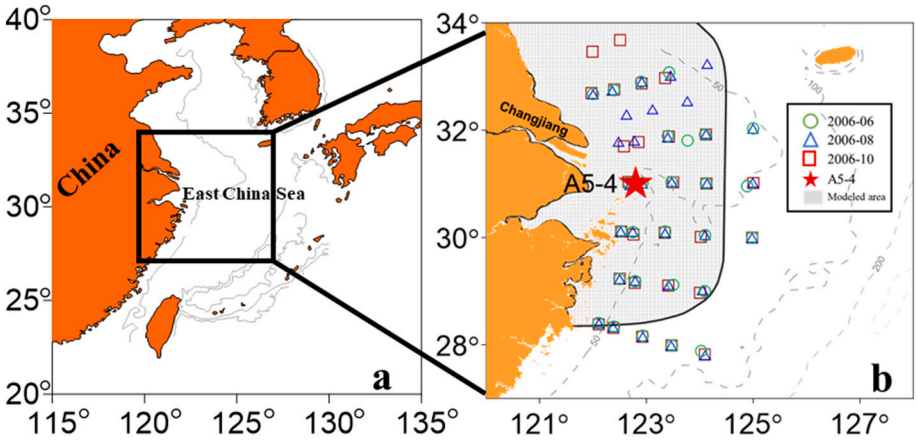

Fig. 1. (a) Study area. (b) Sampling stations and modeled area in this study. The star indicates where core A5-4 was collected.

^{137}Cs methods, and grain size and organic carbon contents were determined and published previously (Liu et al., 2019). There is an error of a few years in sediment core dating (Liu et al., 2019; Sanchez-Cabeza and Ruiz-Fernández, 2012). Out of the three cores, we finally chose the core A5-4 in this work, which showed the best dating result and hence likely best sedimentation and preservation status (Liu et al., 2019). The time resolution of core A5-4 has been described by Liu et al. (2019). Briefly, the lowest sedimentation rate (0.22 cm yr-1) occurred at the top of the sediment after 1984. A relatively higher sedimentation rate (0.69 cm yr-1) was found between 1984 and 1970. The highest sedimentation rate (2.47 cm yr-1) was observed prior to 1970s.

2.3. Phytoplankton community structure quantification

The phytoplankton community structure in the surface waters (as a contribution to total Chla) was estimated via CHEMTAX on the basis of pigment data (Mackey et al., 1996). Given the study area, diatoms, dinoflagellates, cyanobacteria, haptophytes, prochlorophytes, chlorophytes, prasinophytes, cryptophytes and chrysophytes are considered. Input pigment ratios were chosen from previously published work in similar regions of the Changjiang Estuary or ECS (i.e., the Changjiang Estuary and ECS; Furuya et al., 2003a; Zhu et al., 2009), and the ratios for prochlorophytes were from Mackey et al. (1996) (Table S2). CHEMTAX is not applied to pigments in near-bottom waters or sediments. Four successive CHEMTAX runs were performed to improve output estimates (Wang et al., 2015).

For sedimentary pigment, the diagnostic pigment ratio is used to reflect the relative biomass shift in history [e.g., peridinin (dinoflagellates) vs. fucoxanthin (diatoms)]. The relation between pigment ratio (e.g., the peridinin/fucoxanthin ratio) and phytoplankton biomass ratio (e.g., the dinoflagellates/diatoms ratio) was checked and verified by water column investigations (see Fig. S3) and the literature (Liu et al., 2014).

2.4. Historical data and numerical modeling

The yearly variation in the biogeochemistry of the Changjiang Estuary and offshore areas (Fig. 1b) was simulated by 3D modeling based on the finite-volume community ocean model (FVCOM) and the European regional seas ecosystem model (ERSEM). The FVCOM is an unstructured-grid, 3D, finite-volume ocean model that includes physical modules for waves, currents, and sediments (Chen et al., 2013). The triangular grid used in the FVCOM provides excellent matching for complex coastlines, islands, and steep channels, which makes it suitable for coastal modeling. The ERSEM is one of most comprehensive and established biogeochemical and ecosystem models for low-trophic-level marine food webs, including marine pelagic and benthic systems (Butenschön et al., 2016). The two models have been successfully coupled and applied to the Changjiang Estuary with the inclusion of the multiple driving factors of river discharge and coastal and ocean circulation on seasonal to decade timescales (Ge et al., 2020a; Ge et al., 2020b). In this study, the FVCOM–ERSEM system was applied for the 1960–2018 period incorporating multiple forces, including river flux, atmospheric forcing, and ocean circulation. The wave and sediment modules were activated to reveal turbidity dynamics for light penetration in the water column. Measured freshwater discharges and historical nutrient records for the upstream river boundary at Datong station were applied, with this being the closest hydrological station to the estuary. Monthly river freshwater discharges from 1960 to 1994 were applied, and daily values were applied from 1995 to 2018. Nutrient data were obtained from published sources (Dai et al., 2010; Ding et al., 2019; Zhu et al., 2009; Zhu et al., 2014). Atmospheric forcing statistics for surface radiation and wind were provided by the National Centers for Environmental Prediction (NCEP)–National Center for Atmospheric Research (NCAR) Reanalysis 1 for 1960–1979 and the European Center for Medium-Range Weather Forecasts (ECMWF)-ERA dataset for 1980–2018. The SST was assimilated in the model with multiple remote sensing data, including AVHRR and MODIS, whenever available (i.e., after 1979). The lateral boundary is configured as climatological condition of intrusion of Kuroshio and Taiwan Warm Current. That is, the open ocean settings remain constant seasonal cycles during the entire modeled time period (1960–2015).

In addition to real scenarios run with historical riverine nutrient data, two additional 'virtual' scenarios were also tested, namely, the DIP-decrease and DIP-increase runs. For the former, the DIP output from the Changjiang River for 1980–2018 was set as 40% of the historical value used in the real scenario; for the latter, it was set as 2.5 times the historical value. For the remaining parameters (e.g., DIN), the virtual and real scenarios were the same.

In the current ERSEM model, the phytoplankton assemblage was composed of four groups of phytoplankton, namely, diatoms, dinoflagellates, nanophytoplankton, and picophytoplankton (Butenschön et al., 2016). There was a slight difference in phytoplankton community definition between the water column investigation and the model, but the key groups (diatoms and dinoflagellates) concerned were the same.

3. Results

3.1. The surface and bottom waters

For the entire study area, the monthly pigment concentrations and derived phytoplankton assemblages are briefly shown in Tables S3 and S4, respectively. The surface distribution patterns for pigment and phytoplankton assemblages can further be found in the supplemental

materials (Figs. S4-S9).

At site A5-4, Chla showed seasonality, with the biomass in August (7.6 ± 1.8 μg L^{-1}, $n = 2$) as the maximum, followed by that in October (3.2 μg L^{-1}, $n = 1$) and June (1.6 ± 0.8 μg L^{-1}, n = 2). In August, when phytoplankton biomass was high, FUCO (diatoms) and PER (dinoflagellates) were the most abundant diagnostic pigments at site A5-4, being an order of magnitude higher than other diagnostic pigments such as HEX (haptophytes), ZEA (cyanobacteria), and ALLO (cryptophytes). ZEA can even be below the detection limit (June; Table S3). For June and October, compared to other pigments, FUCO remained the dominant diagnostic pigment at site A5-4.

Spatially, FUCO and PER always tend to prevail in near-shore waters, whereas ZEA is usually concentrated offshore (e.g., water depth > 50 m) (Figs. S4-S6). Accordingly, diatoms were the largest Chla contributor at site A5-4 in all three months (70% in June, 50% in August and 80% in October; Figs. S7-S9). Dinoflagellates and prasinophytes were the second largest Chla contributors at site A5-4, but both were several times lower in contribution. Cyanobacteria usually contributed <3% of the total Chla at site A5-4 (Figs. S7-S9).

Of the entire investigated area, pigment concentrations in near-bottom waters were usually lower than those at the surface (Table S3; Fig. 2). In June, when the PER concentration in surface water was at its highest (~8 μg L^{-1}), its concentration in near-bottom waters increased to a similar concentration, increasing with surface PER concentrations (Fig. 2b). This pattern is particularly clear for shallow sites (depth < 40 m including site A5-4; Fig. 2b). In August, diatom blooms occurred (e.g., surface FUCO over ~16 μg L^{-1}), but the corresponding FUCO concentration in near-bottom waters was usually <3 μg L^{-1} (Fig. 2c), suggesting poorer coupling (lower r^2) relative to peridinin. Overall, the coupling of surface-bottom PER concentrations was the best ($r^2 = 0.77$, $p < 0.01$; Fig. 2b), while the correlations of Chla and other diagnostic pigments (FUCO, ALLO, HEX and ZEA) were significantly lower than that of PER (Fig. 2a, c-f). Furthermore, the slope of PER is the biggest (0.73; Fig. 2b), suggesting that the elevated surface PER concentration can be more efficiently transported to the near-bottom waters than other phytoplankton pigments (Fig. 2 c-f). The surface-bottom coupling of pigments showed no relation with the water column physical parameters (figure not shown).

3.2. The sediment core A5-4

Dating of core A5-4 has been published elsewhere (Liu et al., 2019). Briefly, the dating is based on $^{210}Pb_{ex}$ and ^{137}Cs, which indicates a sedimentation rate of 0.22 cm yr^{-1} at 0–7 cm depth, 0.69 cm yr^{-1} at 7–17 cm depth, and 2.43 cm yr^{-1} at 17–181 cm depth.

The preserved pigment decreased from top to bottom (young to old) for all pigments (Fig. 3). In the core, Chla was higher in the top 6 cm (1990–present), with a maximum (3.7 μg g^{-1} OC) occurring at 5 cm (1993), followed by a decrease until the early 1980s. Another Chla peak can be found in the middle 1970s, with an overall downward decrease to the 1960s (Fig. 3a). Before the 1960s, Chla remained at a very low concentration. Chlb (0.3 μg g^{-1} OC to 5.7 μg g^{-1} OC) showed a similar pattern like Chla, with the maximum (5.7 μg g^{-1} OC) occurring at 4 cm (1998). FUCO (<0.1 μg g^{-1} OC to 2.3 μg g^{-1} OC) overall followed the pattern of Chla (Fig. 3a), with the maximum (2.3 μg g^{-1} OC) also being detected at 5 cm (1993). PER showed a similar concentration range as FUCO but with more fluctuations (peaks). The coupling of PER and Chla existed in almost every layer where PER peaks were found. For example, five PER peaks can be found in the approximate years 1903, 1946, 1960, 1967, and 1975 (see arrows in Fig. 3a). For all five PER peaks, Chla also showed elevated concentrations (or peaks) during the same period of time (Fig. 3a).

In the water column, ZEA and ALLO had order-of-magnitude lower concentrations than Chla, FUCO, and PER (Table S3), but the ZEA and ALLO concentrations in the core showed the opposite pattern; namely, their concentrations were higher than those of sedimentary FUCO, PER, and Chla (Fig. 3). ZEA ranged from 1.2 μg g^{-1} OC to 6.1 μg g^{-1} OC, and ALLO ranged from 0.5 μg g^{-1} OC to 3.6 μg g^{-1} OC in the core. This

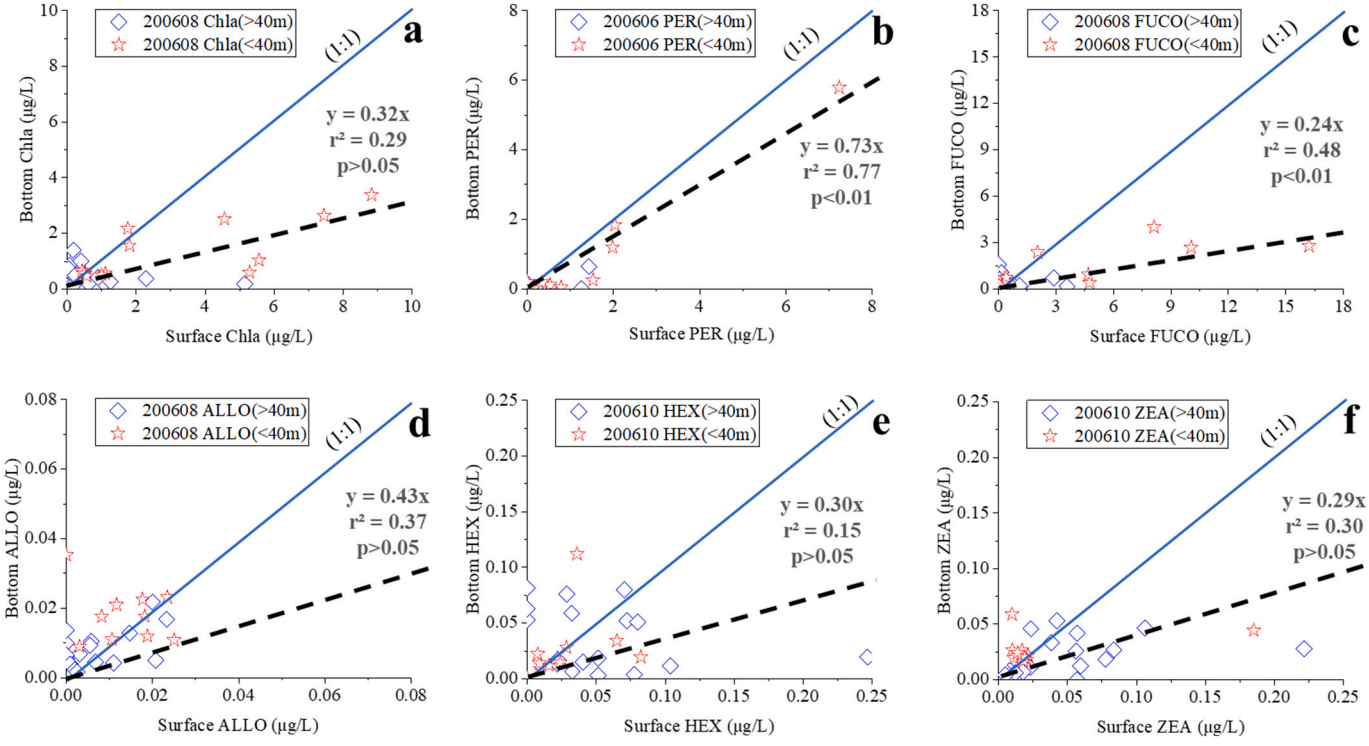

Fig. 2. Selected pooled surface and bottom pigment concentrations for (a) Chla in August; (b) PER in June; (c) FUCO in August; (d) ALLO in August; (e) HEX in October; and (f) ZEA in October 2006. The solid line represents a 1:1 relationship; dashed lines represent the linear regression. (40 m refers to the depth of the station).

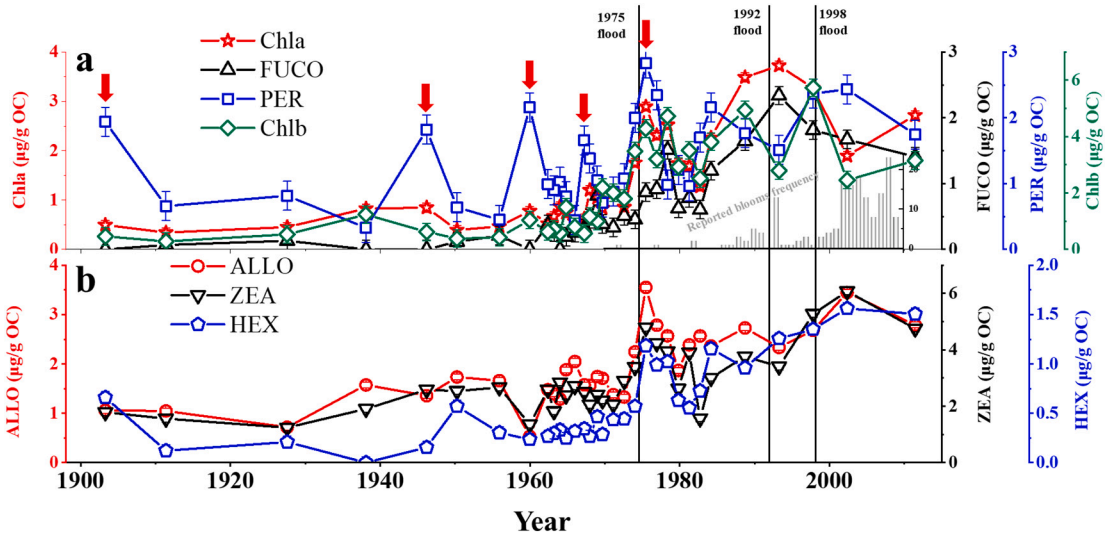

Fig. 3. Preserved pigment concentration (μg g^{-1} OC) in core A5-4. The arrows indicate the 5 PER peaks where elevated Chla also co-occurred at approximately the same time. The organic carbon content in core A5-4 is cited from the literature (Liu et al., 2019). The black line shows several severe flooding events in China in recent decades. The grey bars show the reported blooms frequency in the Changjiang Estuary and adjacent water. The reported blooms frequency is cited from literature (Liu et al., 2013).

suggests the relative accumulation of ZEA, ALLO and HEX in the sediment. In the late 1970s, when Chla and PER showed a peak (Fig. 3a), all other diagnostic pigments, excluding FUCO, also showed a peak (Fig. 3b).

The total Chla-derivatives (the term Chla-derivatives refers to pheophytin-a, pheophorbide-a, and chlorophyllide a in this work) generally decreased from the top to the bottom of the core, ranging from undetectable to 14.7 μg g^{-1} OC. The Chla/Chla-derivatives ratios in the core ranged between 0.2 and 2.0 (Fig. 4). Two peaks, one at 18 cm (1969) and the other at 25 cm (1966), can be identified with Chla/Chla-derivatives ratios as high as 2.0 and 1.4 (Fig. 4).

3.3. Numerical modeling

The 3D physical-biogeochemical model incorporated the entire Changjiang Estuary and adjacent ECS (Fig. 1b), but here, we focus only on the region of site A5-4 to be more concise.

The simulated Chla ranged between 1.4 and 2.9 μg L^{-1}, and a gradual increase from the late 1970s was simulated (Fig. S10). Overall, the simulated Chla interannual variability agrees with the observation data derived from remote sensing (Fig. S10). Seasonally, simulated Chla was always higher during April–October and remained depleted in winter (Fig. S11). The annual average diatoms/(diatoms+dinoflagellates) ratio shows no clear trend from 1960 to 2012, but the monthly ratio in May begins to decrease from 1991 (Fig. 5a). At the same time, there is an increase of average value of SST in April and May since early 1990s (Fig. 5b).

With respect to the virtual scenarios, the simulated DIP concentration at site A5-4 increased by 20% (river input set as 2.5 times higher riverine DIP than historical real DIP data) and decreased by 8% (river input set at 40% of historical real riverine DIP data) when compared to the real data scenario. Note that the virtual scenarios indicates the impact of changed N/P ratio to the estuarine system. While the estuarine site (A5-4) DIP variation is not as large as the corresponding riverine input endmembers, changes in riverine N/P ratio input indeed caused a change in the N/P ratio and thus the corresponding diatom proportion changes at site A5-4. Namely, a lower N/P ratio (Fig. S12) corresponds to higher diatom proportions at site A5-4 and vice versa (Fig. 6).

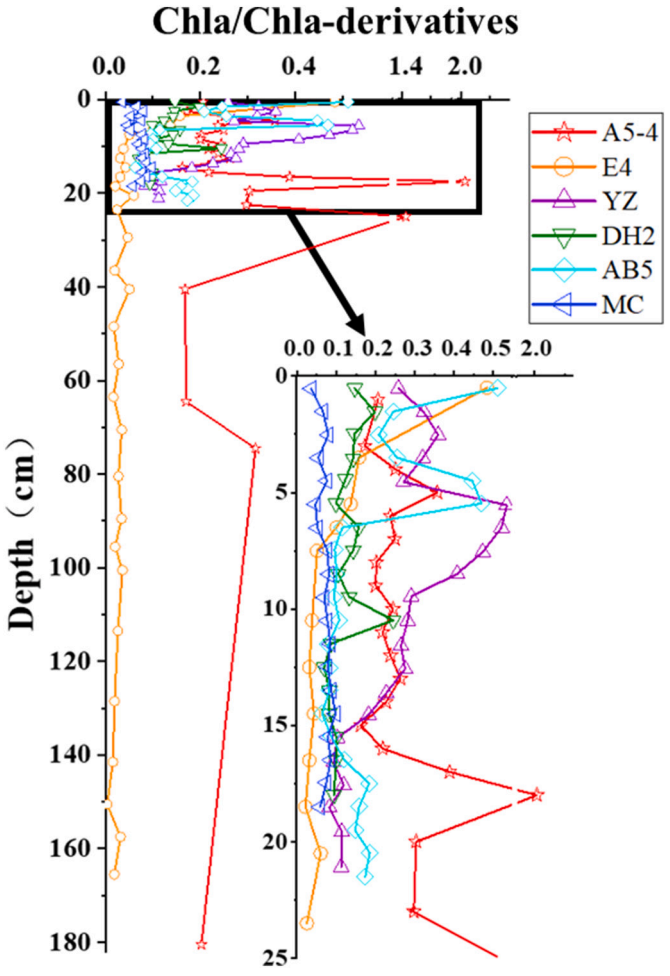

Fig. 4. Chla/Chla-derivatives ratios in the core A5-4. Ratios of other cores from the ECS are also shown. Data sources: E4, Zhu et al. (2014); YZ, Zhao et al. (2012); DH2, Zhao et al. (2012); AB5, Zhao et al. (2012); MC, Zhao et al. (2012).

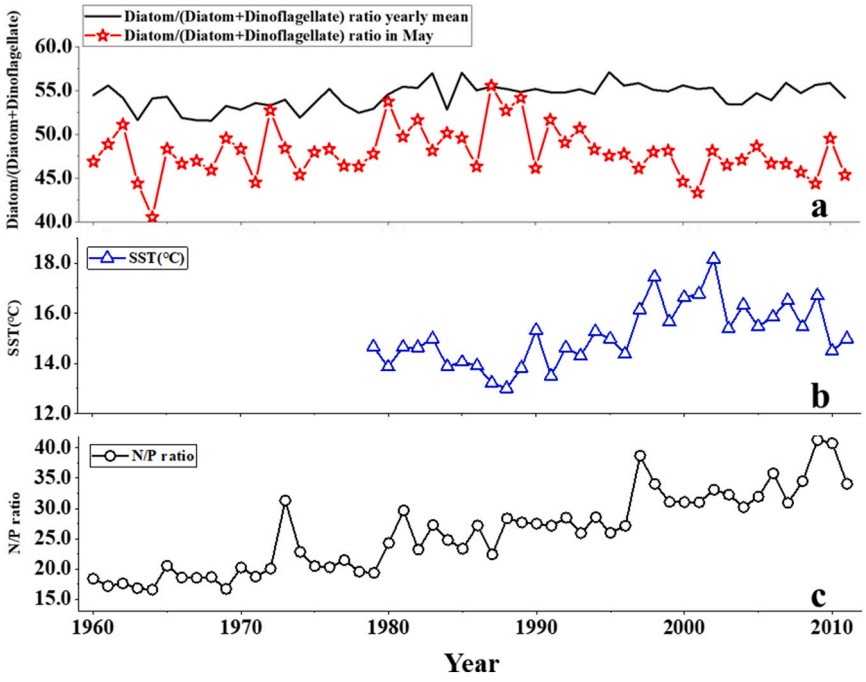

Fig. 5. The model result for site A5-4 of its a) Modeled diatoms/(diatoms+dinoflagellates) ratio in surface waters; b) average value of SST in April and May; and c) surface N/P ratio in April and May. Note that the SST was assimilated in the model with multiple remote sensing data since 1979 when remote sensing data is available.

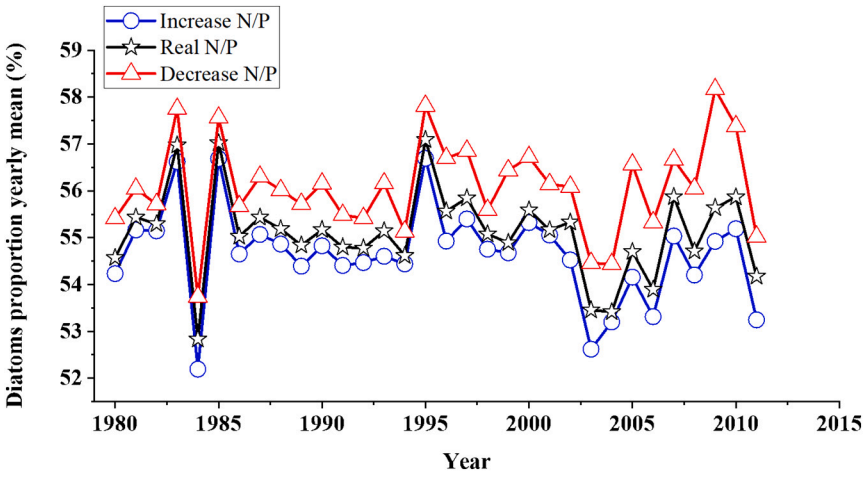

Fig. 6. Modeled diatom proportion in the total phytoplankton biomass in surface water at site A5-4. Decreased and increased N/P relate to two virtual scenario runs. To achieve the decreasing or increasing N/P ratio, the riverine DIP is set as decreased to 40% of the historical recorded value (DIN not changed, hence increasing N/P) and as increased to 2.5 times the historical recorded value (DIN not changed, hence decreasing N/P), respectively. Real N/P is the model result with riverine nutrient concentration at the historical recorded level.

4. Discussion

4.1. Key phytoplankton groups evidence in core A5-4

The Chla/Chla-derivatives ratio is influenced by many factors, including grazing activities and sediment preservation (Carpenter et al., 1986; Collos et al., 2005), and the ratio can reflect pigment preservation in the sediment (Reuss et al., 2005; Zhao et al., 2012). Though the grazing effect may interfere with the relation, it is usually expected that a higher Chla/Chla-derivatives ratio indicates better preservations, given that the denominator Chla-derivatives are more stable than the parent Chla (Reuss et al., 2005; Zhao et al., 2012). The Chla/Chla-derivatives ratio in core A5-4 is comparable or even higher than that in other cores in similar regions (Fig. 4), suggesting that pigment preservation in core A5-4 is acceptable. The two outliers at depths of 18 and 25 cm, with extremely high Chla/Chla-derivatives ratios (Fig. 4), may be due to a decrease of the grazing effect (Strom, 1993; Turner, 2015).

In the 1990s and 2000s, the increased frequency of blooms in the Changjiang Estuary and adjacent area was accompanied by a rapid increase in the concentration of preserved pigments in the sediment (Fig. 3a). As for the flood in 1975, 1992 and 1998, clear record can be identified in core A5-4, with several pigments sub-peaks (Fig. 3a). Although preserved ZEA and ALLO were clearly higher in concentration than FUCO (Fig. 3), diatoms (FUCO), not ZEA (cyanobacteria) or cryptophytes (ALLO), were the key Chla contributors in the water column (Table S4; Figs. S7-S9). Hence, judging the key phytoplankton groups based only on raw sedimentary pigment data could sometimes be misleading. The reason behind this may be due to different chemical stabilities among these labile pigment compounds (Reuss, 2005). A similar contrasting pigment concentration between FUCO and ZEA has been previously reported (Li et al., 2011).

Early diagenetic processes occur when organic matter is buried in the sediment, and the process can be quantitatively expressed as (Berner, 1980; Stephens et al., 1997):

$$y = y_0 e^{-kt} \quad (1)$$

where y_0 is the initial concentration (μg g^{-1} OC), k is the degradation constant (yr^{-1}), and t is time (yr). Here, we accordingly apply this model (Eq. (1)) to the sediment core pigment data, with the degradation constants k and r^2 shown in Table 1. The k of 0.017 yr^{-1} for Chla in core A5-4 is small in contrast to that in another core E4 (1.03 yr^{-1}), which was also collected off the Changjiang Estuary (Zhu et al., 2014). The different k values between A5-4 (this study) and E4 (Zhu et al., 2014) indicate the different Chla degradation rates. The smaller k value at A5-4 means a longer half-life and hence better storage condition (Zhu et al., 2014) than that at E4. This is consistent with the Chla/Chla-derivatives ratio patterns, in which core A5-4 has higher Chla/Chla-derivatives ratios than the E4 core (Fig. 4). Similar models are further applied to FUCO, ALLO, and ZEA, which also yield lower k values than the corresponding pigments in E4.

For the model results (Table 1), while the other pigments all show good relations ($r^2 > 0.5$), the r^2 for PER is very poor ($r^2 = 0.16$) (Table 1), suggesting that such early diagenetic processes may not apply for PER. However, if the five PER peaks (1903–1975; Fig. 3a) are not considered, a much better model performance can be achieved ($r^2 = 0.41$ relative to $r^2 = 0.16$; Table 1). The possible reasons include the unique surface-bottom coupling patterns of PER relative to the remaining diagnostic pigments as revealed by water column investigations (Fig. 2). Again, among all pigments, only PER showed good surface-bottom concentration coupling (Fig. 2b), which suggests that bottom PER tends to show a prompt response to surface PER under high concentration scenarios (Fig. 2b). For the remaining diagnostic pigments, however, such a prompt response under high concentration seems absent (Fig. 2 c-f). Although there were additional processes before the pigment was finally buried into the sediment, it is reasonable to expect that the peaks of PER (e.g., 1903, 1946, 1960, 1967, and 1975; Fig. 3) were the result of corresponding intense dinoflagellate growth (blooms) at that time, and the high PER sinking load during these potential bloom periods interfered with the normal pigment burial rhythm and further resulted in different early diagenesis processes (e.g., degradation following a different k), whereas for the remaining diagnostic pigments, the generally poor surface-bottom coupling in the water column (Fig. 2 c-f) reduced any intensive bloom impact if there were any (Fig. 3 a&b).

Based on the pigment degradation model (Eq. (1) and Table 1), the term pigment anomaly (in μg g^{-1} OC) is defined as the difference between the observed sedimentary pigment and the corresponding model fitting result for that layer. The pigment anomaly concentration reflects the deviations (excess or deficiency) of the pigments at given layers from the surface sediment layer (i.e., concentration in 2011). As a result, differences in pigment stabilities play a minor role when comparing the pigments anomaly because the early diagenetic effect has been eliminated by the model.

The higher preserved ALLO and ZEA in the sediment (when compared to FUCO) showed a much poorer relation with Chla when checking for its anomaly ($r^2 = 0.26$ for ALLO, $r^2 = 0.14$ for ZEA, $r^2 = 0.63$ for FUCO; Fig. 7). Indeed, the relation between FUCO anomaly and Chla anomaly ($r^2 = 0.63$; Fig. 7a) was the strongest among all diagnostic pigments (Fig. 7), indicating that the variation in diatoms (FUCO), instead of other algae, plays a dominant role in determining the variation in total phytoplankton biomass (Chla). This sedimentary pattern (Fig. 7) hence suggests that diatoms are the dominant phytoplankton biomass contributor, which agrees with water column observations (Table S4).

While diatoms played a dominant role in determining the total phytoplankton biomass (Table S4; Fig. 7a), there are studies reporting a shift from diatoms-dominated to dinoflagellates-dominated blooms in spring (especially in May) in recent decades, but with different time windows (Jiang et al., 2014; Liu et al., 2013; Ou et al., 2014; Tang et al., 2006). Here, evidence from sediment core A5-4 provides another opportunity to address this question, as is discussed below.

Table 1
Degradation model (Eq. (1)) constant k and relation (r^2) for the key diagnostic pigments in core A5-4. The value* is achieved by excluding the 5 PER peaks (i.e., 1903, 1946, 1960, 1967, and 1975).

Pigment	k	r^2
Chla	0.017	0.5
FUCO	0.022	0.52
PER	0.007(0.010*)	0.16(0.41*)
ZEA	0.013	0.54
ALLO	0.01	0.5
HEX	0.025	0.67

4.2. The time window of the shift in spring blooms

Certain species of haptophytes and chrysophytes also contain fucoxanthin, but even total haptophytes and chrysophytes make very trace contribution to total Chla in our study site when compared to diatoms (Furuya et al., 2003b; Jiang et al., 2014). As for the outlier dinoflagellates *Karenia mikimotoi*, which contains FUCO instead of PER (Zapata et al., 2012), it also plays a limited role when compared to other dinoflagellates and diatoms. For example, in the total 174 times of recorded blooms off the Changjiang estuary from 1972 to 2009, the *Karenia mikimotoi* was recorded for only 3 times, while the top three bloom contributing species are *Prorocentrum donghaiense* (38 times), *Skeletonema costatum* (35 times), and *Prorocentrum dantatum* (15 times) as a comparison (Liu et al., 2013). Given the most common phytoplankton species, namely *Skeletonema costatum* (diatoms), *Prorocentrum donghaiense* (dinoflagellates), and *Prorocentrum dantatum* (dinoflagellates) (Liu et al., 2013) all follow the diagnostic pigment distribution pattern (fucoxanthin in diatoms and peridinin in dinoflagellates), applying PER and FUCO to reflect dinoflagellates and diatoms involves no big problems.

To calibrate the early diagenesis effect (Table 1), we define another term, namely, the original pigment (in μg g^{-1} OC), for every sediment layer. Namely, by regarding the observed pigment concentration at a certain layer as y in Eq. (1), with the known k and t at that certain layer (Table 1), the solution y_0 is the original pigment concentration for that layer. This term removes the corresponding early diagenesis effect for that individual pigment and reconstructs the historical pigment concentration at the time of that layer.

Overall, the original-PER/original-FUCO ratio has undergone a gradual decrease from the past (bottom) to the present (top) of the sediment (Fig. 8). Due to the strong relationship between PER/FUCO and dinoflagellates/diatoms biomass ratios (Fig. S3), the pattern revealed in Fig. 8 indicates that the diatoms abundance has increased in recent decades relative to dinoflagellates. However, while the overall decreasing pattern is clear, there is a turning point in the layer corresponding to 1990s, after which the original-PER/original-FUCO ratio increases (Fig. 8), suggesting that dinoflagellates began to increase in 1990s, relative to diatoms.

The burial of phytoplankton pigments into the sediment involves complex biogeochemical processes, including decomposition and sinking efficiency in the water column, burial in surface sediment (Arndt et al., 2013) and decomposition products of fucoxanthin and Chla further indicate complex early diagenesis process in the sediment (e.g., Chen et al., 2003), all of which introduce uncertainties. While the early diagenesis process for PER and FUCO in the sediment is quantitatively solved via model (Eq. (1)), water column investigations reveal different surface-bottom pigment concentration coupling features between PER and FUCO. In the water column, PER (dinoflagellates) shows better sinking efficiency under higher surface PER concentrations (Fig. 2b), whereas FUCO tends to have a better surface-bottom concentration coupling under low surface FUCO concentrations (Fig. 2c). The sinking rate of dinoflagellates during the bloom event was 12 ± 2 m d^{-1}, which

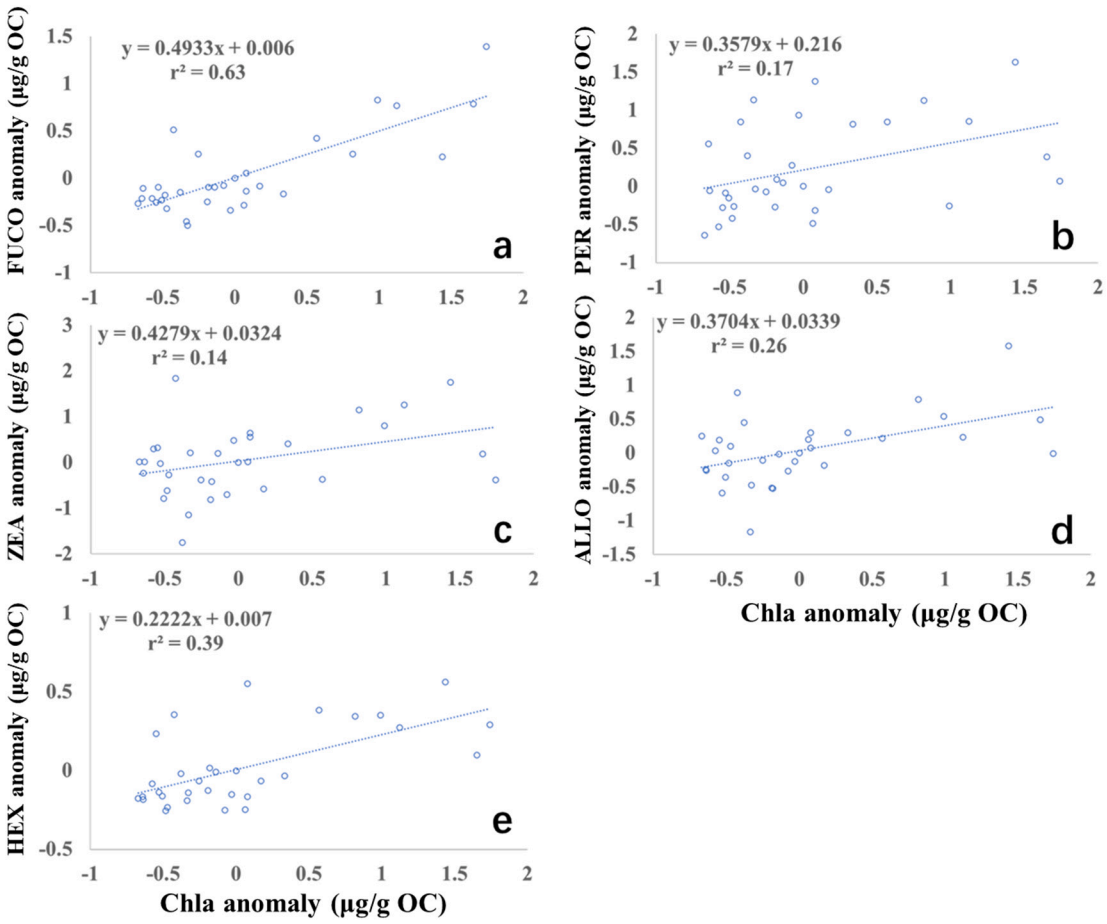

Fig. 7. The defined Chla anomaly plotted against a) FUCO anomaly, b) PER anomaly, c) ZEA anomaly, d) ALLO anomaly and e) HEX anomaly. The pigment anomaly concentrations are calculated as observed sedimentary pigment concentrations subtracted from corresponding modeled concentrations. For details, see Section 4.1.

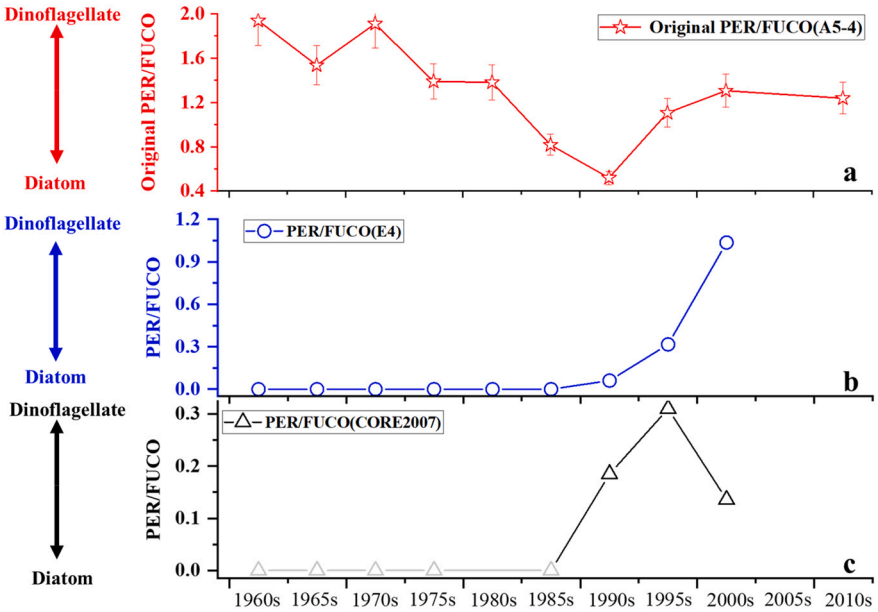

Fig. 8. The PER/FUCO ratio in core (a) A5-4, (b) E4, and (c) core2007. The core E4 is cited from Zhu et al., 2014 and core 2007 is cited from Li et al., 2011a. PER is the key pigment for dinoflagellates and FUCO is the key pigment for diatoms. Note y-axis ranges are different among the three subplots.

was more than 10 times the rate at non-bloom stations (1.0 ± 0.8 m d^{-1}) (Qiu et al., 2018) and microscopic observations indicated that the formation of aggregates by the *Prorocentrum donghaiense* (the dominant phytoplankton species; a kind of dinoflagellates) enhanced the sinking rates during the bloom (Qiu et al., 2018). This means that different algal blooms likely have different impacts on sinking signals, and

dinoflagellate blooms had a stronger impact on sedimentary pigment records than diatom blooms. Therefore, the water column findings (Fig. 2) suggest that the PER/FUCO ratio shift in the early 1990s (Fig. 8) can be due to increased dinoflagellate blooms since the early 1990s. This idea is consistent with water column observations, which suggests that the shift between diatoms and dinoflagellates is more likely a seasonal event (e.g., succession during spring blooms) (Liu et al., 2013; Tang et al., 2006).

Our work is further compared with previous sedimentary pigment works that also conducted off the Changjiang Estuary and adjacent ECS (Bao et al., 2010; Kang et al., 2016; Li et al., 2011; Zhao et al., 2012). Among these works some studied detected or showed PER and FUCO, and we hence pooled all available sedimentary PER and FUCO in previous work (Li et al., 2011; Zhu et al., 2014)(Fig. 8b&c) to check for the trend that recorded in sediment. Indeed, an increase of PER/FUCO occurred roughly in 1990s can be identified (Fig. 8b&c), which is consistent with our findings from core A5-4. The selected core A5-4 showed much better burial and preservation of pigments relative to core E4 and core 2007 (e.g., much higher Chla/Chla-derivatives ratio; Fig. 4) and accordingly a more detailed variation of PER/FUCO prior to 1990s can be found (Fig. 8a) when compared to other cores (Fig. 8b&c). The absolute PER/FUCO ratio values in core A5-4 were the highest in the three cores (0.2–0.8 vs. <1.0 or <0.3; Fig. 8), which can be largely attributed to the less stability of PER relative to FUCO (Leavitt and Hodgson, 2002) (Fig. 8a vs. Fig. 8b & c). In the south of the Changjiang Estuary, studies of core pigments have also revealed succession between diatoms and dinoflagellates (Abate et al., 2017). There were some differences in PER/FUCO between the two studies, which could be attributed to the distance between the two study areas, differences in the frequency and timing of the blooms (Xiao et al., 2019). In addition to pigments, some other sedimentary proxies are also used in this region. Based on sedimentary sterols (brassicasterol+dinosterols), it is suggested that the contribution from diatoms decreased relative to dinoflagellates in 1992 (Guo et al., 2020; Xing et al., 2016).

4.3. The 3D model and potential mechanism behind diatoms-dinoflagellates shift

Overall, the FVCOM–ERSEM model has proven to be robust and yields reasonable outputs (Ge et al., 2020a; Ge et al., 2020b). The modeled Chla concentration off the Changjiang Estuary exhibits an increasing trend after 1980 (Fig. S10), consistent with field observations (Wang, 2006; Yang et al., 2014). Seasonally, modeled Chla concentrations show elevated levels in spring, summer, and early autumn, with a sharp drop to minimum levels in winter (Fig. S11), which is also consistent with field observations (Liu et al., 2013; Shen et al., 2019).

The simulated result suggests that the diatoms contribution relative to dinoflagellates on annual scale shows no clear interannual trend from 1960 to 2012, but the diatoms contribution in May began to decrease in approximately 1990 (Fig. 5), and May is the month with the highest bloom frequency (Liu et al., 2013; Tang et al., 2006). The decreasing diatoms in May are consistent with field observations (Yu et al., 2017). The modeled time point at which spring diatoms started to decrease (~1990; Fig. 5a) is consistent with the core result (early 1990s; Fig. 8a). Furthermore, numerical modeling indicates that the decrease in diatom blooms (increase in dinoflagellate blooms) in May rather than an annual decrease in diatoms biomass (Fig. 5) causes the increase in the sedimentary original PER/original FUCO ratio in the 1990s (Fig. 8a), which is consistent with field phytoplankton observations (Guo et al., 2014; Yu et al., 2017). In the water column, PER showed higher sinking efficiency during blooms, relative to diatoms (Fig. 2), and this also suggest the change in sedimentary original PER/original FUCO ratio in early 1990s (Fig. 8a) should be due to increased dinoflagellate blooms, rather than a general biomass increase all year round.

The role of increasing temperature in dinoflagellates ascend has been suggested from studies that based on multi-year observations (e.g., Jiang et al., 2014; Liu et al., 2016; Xiao et al., 2018). In the modeling result, the correspondence between spring SST increase and diatoms drop is more obvious, or dominant, than the correspondence between spring N/P ratio and shift in diatoms-dinoflagellates (Fig. 5abc). While the spring SST showed a clear increase since early 1990s, the SST showed no interannual variation if all-year mean SST is considered (figure not shown). Hence, our model further suggests that it is the spring SST that plays a role in the diatoms-dinoflagellates shift (Fig. 5b&8a). At the site A5-4, the SST after June was usually over 20 °C, whereas in May the SST was lower than 20 °C (Fig. S13). When under 20 °C (in spring in our case), dinoflagellates show much stronger positive growth tendence with increasing temperature relative to diatoms, whereas when temperature is over 20 °C (in summer and fall), dinoflagellates in turn show varied but overall negative response to increasing temperature (Liu et al., 2016).

In addition to temperature, nutrient is another factor that frequently mentioned in literature for its role in diatoms-dinoflagellates shift (Li et al., 2014; Liang et al., 2019; Lu et al., 2022; Zhou et al., 2017a). At site A5-4, there is no significant N/P ratio increase in the period of early 1990s and instead a fluctuated but continuously increasing pattern is suggested from 1960s to 2010s (Fig. 5c). While there is a lack of well correspondence between N/P increase and diatoms drop in the early 1990s (Fig. 5a&c), the model virtual runs indicates that a reduction in riverine DIP input which exacerbated the P limitation reduces the diatom proportion in total phytoplankton biomass, whereas an increase in DIP input causes an increase in the diatom proportion (Fig. 6).

Physiologically, dinoflagellates respond more directly and rapidly to temperature rise, relative to diatoms (Feng et al., 2021), while competition between diatoms and dinoflagellates is largely determined by their differences in DIP utilization (Egge, 1998). The combination of both model results (Fig. 5c&6) further indicates that the effect of increasing spring SST and increasing N/P ratio on the diatoms-dinoflagellates shift is dominant and recessive, respectively.

Besides SST and riverine output, the open ocean serves as another important nutrient source for the ECS (Chen, 1996; Yang et al., 2013; Zhang et al., 2019; Zhang et al., 2018). Eventually, Kuroshio waters are reported as important nutrient sources that trigger near-shore spring phytoplankton blooms (Yang et al., 2018; Zhao et al., 2019). Zhou et al. (2017a) suggested that diatom blooms are more closely related to terrestrial input, with intrusion of Kuroshio waters being more important to dinoflagellate blooms. In addition to direct nutrient supply, the intrusion of the Kuroshio also changes the strength of stratification within the water column and the depth of the mixed layer. These factors will further affect the irradiance environment and the competition between diatoms and dinoflagellates. In our model the lateral boundary is configured as climatological condition and hence impact from open ocean like Kuroshio needs further study.

5. Conclusion and perspective

Preserved sedimentary pigments are useful proxies for reconstructing phytoplankton history, especially for periods when intensive direct observation or instrumental records are lacking. The key finding of this work is the reconstructed diatoms-dinoflagellates shift over the past decades. In this work, we present evidence for the time window of the diatoms-dinoflagellates shift in the early 1990s. Based on surface-bottom concentration coupling features in the water column, as well as the numerical modeling test, we further propose that the mechanism behind this PER/FUCO shift is the increasing spring dinoflagellate blooms instead of a simple diatoms (dinoflagellates) biomass decrease (increase).

Our work demonstrates the importance of conducting water column proxy investigations and removing early diagenesis effects before reconstructing phytoplankton patterns via sedimentary data. A simple comparison of sedimentary pigments would easily induce the incorrect conclusion that cyanobacteria and cryptophytes, rather than diatoms,

are the dominant phytoplankton groups in the water column. With the organic matter degradation model, we successfully reconstructed the key phytoplankton contributor (diatoms), and the PER/FUCO ratio was free from such interference. Another important finding from water column investigations is the different surface-bottom pigment concentration couplings or how the near-bottom pigments reflect the surface concentrations. This knowledge is helpful in interpreting the PER/FUCO ratio shift in the early 1990s, which supports the idea that increasing dinoflagellate blooms may be the mechanism responsible, instead of a simple diatoms (dinoflagellates) biomass decrease (increase).

The mechanism for the diatoms-dinoflagellates shift in spring blooms is an interesting topic, which is a question that ranges from molecular to ecosystem scales. Based on core A5-4 and a physical-biogeochemical 3D model, we present evidence for the shift time window (early 1990s) and suggest that the effect of increasing spring SST and increasing N/P ratio on the diatoms-dinoflagellates shift is dominant and recessive, respectively.

CRediT authorship contribution statement

Fu-Tao Fang: Writing - Original Draft, Analyzed the data, Investigation **Zhuo-Yi Zhu**: Writing - Original Draft, analyzed the data, Conceptualization, Investigation, project administration **Jian-Zhong Ge:** Methodology, Writing - Review & Editing **Bing Deng:** Writing - Review & Editing **Jin-Zhou Du:** Writing - Review & Editing **Jing Zhang:** Writing - Review & Editing.

Declaration of competing interest

The authors declare that they have no known competing financial interests or personal relationships that could have appeared to influence the work reported in this paper.

Acknowledgments

We are grateful to the captains and crew of R/V *Beidou* and R/V *RungJiang,* who helped in collecting water samples and sediment cores. We thank Shen-Yang Shi (SKLEC/ECNU), who participated in the numerical modeling. We are grateful to the anonymous reviewers whose comments improved the original manuscript. This work was supported by the Ministry of Science and Technology of China (No. 2016YFA0600904, 2006CB400601), the National Natural Science Foundation of China (No. 41976042), and the China National Key Research and Development Program (No. 2018YFD0900901). The data concerned in this work have all been shown in the main text (via figures or tables) and supplemental materials.

Appendix A. Supplementary data

Supplementary data to this article can be found online at https://doi.org/10.1016/j.marpolbul.2022.113638.

References

Abate, R., Gao, Y., Chen, C., Liang, J., Mu, W., Kifile, D., Chen, Y., 2017. Decadal variations in diatoms and dinoflagellates on the inner shelf of the East China Sea, China. Chin. J. Oceanol. Limnol. 35, 1374–1386.

Anderson, D.M., Glibert, P.M., Burkholder, J.M., 2002. Harmful algal blooms and eutrophication: nutrient sources, composition, and consequences. Estuaries 25, 704–726.

Arndt, S., Jørgensen, B.B., LaRowe, D.E., Middelburg, J.J., Pancost, R.D., Regnier, P., 2013. Quantifying the degradation of organic matter in marine sediments: a review and synthesis. Earth Sci. Rev. 123, 53–86.

Bao, H.-Y., Wu, Y., Zhu, Z.-Y., Zhang, J., 2010. Distribution of pigments in E 5 core sediments in Changjiang Estuary. Mar. Environ. Sci. 29, 314–316 (in Chinese with English abstract).

Berner, R.A., 1980. Early Diagenesis: A Theoretical Approach. Princeton University Press.

Butenschön, M., Clark, J., Aldridge, J.N., Allen, J.I., Artioli, Y., Blackford, J., Bruggeman, J., Cazenave, P., Ciavatta, S., Kay, S., 2016. ERSEM 15.06: a generic model for marine biogeochemistry and the ecosystem dynamics of the lower trophic levels. Geosci. Model Dev. 9, 1293–1339.

Carpenter, S.R., Elser, M.M., Elser, J.J., 1986. Chlorophyll production, degradation, and sedimentation: implications for paleolimnology1. Limnol. Oceanogr. 31, 112–124.

Chen, C.T., 1996. The Kuroshio intermediate water is the major source of nutrients on the East China Sea continental shelf. Oceanol. Acta 19, 523–527.

Chen, N., Bianchi, T.S., Bland, J.M., 2003. Novel decomposition products of chlorophyll-a in continental shelf (Louisiana shelf) sediments: formation and transformation of carotenol chlorin esters. Geochim. Cosmochim. Acta 67, 2027–2042.

Chen, C., Beardsley, R., Cowles, G., Qi, J., Lai, Z., Gao, G., Stuebe, D., Xu, Q., Xue, P., Ge, J., 2013. An Unstructured Grid, Finite-Volume Community Ocean Model FVCOM User Manual. SMAST. UMASSD Technical Report-13-0701. University of Massachusetts-Dartmouth.

Collos, Y., Husseini-Ratrema, J., Bec, B., Vaquer, A., Hoai, T.L., Rougier, C., Pons, V., Souchu, P., 2005. Pheopigment dynamics, zooplankton grazing rates and the autumnal ammonium peak in a Mediterranean lagoon. Hydrobiologia 550, 83–93.

Dai, Z., Du, J., Zhang, X., Su, N., Li, J., 2010. Variation of riverine material loads and environmental consequences on the Changjiang (Yangtze) Estuary in recent decades (1955–2008). Environ.Sci.Technol. 45, 223–227.

Ding, S., Chen, P., Liu, S., Zhang, G., Zhang, J., Dan, S.F., 2019. Nutrient dynamics in the Changjiang and retention effect in the Three Gorges Reservoir. J. Hydrol. 574, 96–109.

Egge, J., 1998. Are diatoms poor competitors at low phosphate concentrations? J. Mar. Syst. 16, 191–198.

Feng, Y., Chai, F., Wells, M.L., Liao, Y., Li, P., Cai, T., Zhao, T., Fu, F., Hutchins, D.A., 2021. The combined effects of increased pCO2 and warming on a coastal phytoplankton assemblage: from species composition to sinking rate. In: Front.Mar. Sci.8.

Furuya, K., Hayashi, M., Yabushita, Y., Ishikawa, A., 2003a. Phytoplankton dynamics in the East China Sea in spring and summer as revealed by HPLC-derived pigment signatures. Deep-Sea Res. II Top. Stud. Oceanogr. 50, 367–387.

Furuya, K., Hayashi, M., Yabushita, Y., Ishikawa, A., 2003b. Phytoplankton dynamics in the East China Sea in spring and summer as revealed by HPLC-derived pigment signatures. Deep-Sea Res. II 50, 367–387.

Ge, J., Shi, S., Liu, J., Xu, Y., Chen, C., Bellerby, R., Ding, P., 2020a. Interannual variabilities of nutrients and phytoplankton off the Changjiang Estuary in response to changing river inputs. J.Geophys.Res.Oceans 125.

Ge, J., Torres, R., Chen, C., Liu, J., Xu, Y., Bellerby, R., Shen, F., Bruggeman, J., Ding, P., 2020b. Influence of suspended sediment front on nutrients and phytoplankton dynamics off the Changjiang Estuary: a FVCOM-ERSEM coupled model experiment. J. Mar. Syst. 204, 103292.

Guo, S., Feng, Y., Wang, L., Dai, M., Liu, Z., Bai, Y., Sun, J., 2014. Seasonal variation in the phytoplankton community of a continental-shelf sea: the East China Sea. Mar. Ecol. Prog. Ser. 516, 103–126.

Guo, X.-Y., Zhang, H.-L., Li, L., Bi, R., 2020. Biomarker records of phytoplankton productivity and community structure changes in the mud area of the Yangtze River Estuary in the East China Sea during the last 30 years. J. Ocean Univ. China 50, 85–94 (in Chinese with English abstract).

Jiang, Z., Liu, J., Chen, J., Chen, Q., Yan, X., Xuan, J., Zeng, J., 2014. Responses of summer phytoplankton community to drastic environmental changes in the Changjiang (Yangtze River) Estuary during the past 50 years. Water Res. 54, 1–11.

Jiang, Z., Chen, J., Zhou, F., Shou, L., Chen, Q., Tao, B., Yan, X., Wang, K., 2015. Controlling factors of summer phytoplankton community in the Changjiang (Yangtze River) Estuary and adjacent East China Sea shelf. Cont. Shelf Res. 101, 71–84.

Jiang, Z., Chen, J., Gao, Y., Zhai, H., Jin, H., Zhou, F., Shou, L., Yan, X., Chen, Q., 2019. Regulation of spatial changes in phytoplankton community by water column stability and nutrients in the southern Yellow Sea. J.Geophys.Res.Biogeosci. 124, 2610–2627.

Kang, Z., Yu, R., Kong, F., Wang, Y., Gao, Y., Chen, J., Guo, W., Zhou, M., 2016. Records of bulk organic matter and plant pigments in sediment of the "red-tide zone" adjacent to the Changjiang River estuary. Chin. J. Oceanol. Limnol. 34, 915–927.

Leavitt, P.R., Hodgson, D.A., 2002. In: Sedimentary Pigments, Tracking Environmental Change Using Lake Sediments. Springer, Netherlands, pp. 295–325.

Li, X., Bianchi, T.S., Yang, Z., Osterman, L.E., Allison, M.A., DiMarco, S.F., Yang, G., 2011. Historical trends of hypoxia in Changjiang River estuary: applications of chemical biomarkers and microfossils. J. Mar. Syst. 86, 57–68.

Li, H.-M., Tang, H.-J., Shi, X.-Y., Zhang, C.-S., Wang, X.-L., 2014. Increased nutrient loads from the Changjiang (Yangtze) River have led to increased harmful algal blooms. Harmful Algae 39, 92–101.

Liang, Y., Zhang, G., Wan, A., Zhao, Z., Wang, S., Liu, Q., 2019. Nutrient-limitation induced diatom-dinoflagellate shift of spring phytoplankton community in an offshore shellfish farming area. Mar. Pollut. Bull. 141, 1–8.

Liu, L., Zhou, J., Zheng, B., Cai, W., Lin, K., Tang, J., 2013. Temporal and spatial distribution of red tide outbreaks in the Yangtze River Estuary and adjacent waters, China. Mar. Pollut. Bull. 72, 213–221.

Liu, S., Yao, P., Yu, Z., Li, D., Deng, C., Zhen, Y., 2014. HPLC pigment profiles of 31 harmful algal bloom species isolated from the coastal sea areas of China. J. Ocean Univ. China 13, 941–950.

Liu, X., Xiao, W., Landry, M.R., Chiang, K.-P., Wang, L., Huang, B., 2016. Responses of phytoplankton communities to environmental variability in the East China Sea. Ecosystems 19, 832–849.

Liu, Y., Deng, B., Du, J., Zhang, G., Hou, L., 2019. Nutrient burial and environmental changes in the Yangtze Delta in response to recent river basin human activities. Environ. Pollut. 249, 225–235.

Lu, S., Ou, L., Dai, X., Cui, L., Dong, Y., Wang, P., Li, D., Lu, D., 2022. An overview of Prorocentrum donghaiense blooms in China: species identification, occurrences, ecological consequences, and factors regulating prevalence. Harmful Algae 114, 102207.
Mackey, M., Mackey, D., Higgins, H., Wright, S., 1996. CHEMTAX-a program for estimating class abundances from chemical markers: application to HPLC measurements of phytoplankton. Mar. Ecol. Prog. Ser. 144, 265–283.
Milliman, J.D., Meade, R.H., 1983. World-wide delivery of river sediment to the oceans. J. Geol. 91, 1–21.
Mo, Y., Ou, L., Lin, L., Huang, B., 2020. Temporal and spatial variations of alkaline phosphatase activity related to phosphorus status of phytoplankton in the East China Sea. Sci. Total Environ. 731, 139192.
Ou, L., Wang, D., Huang, B., Hong, H., Qi, Y., Lu, S., 2008. Comparative study of phosphorus strategies of three typical harmful algae in Chinese coastal waters. J. Plankton Res. 30, 1007–1017.
Ou, L., Huang, X., Huang, B., Qi, Y., Lu, S., 2014. Growth and competition for different forms of organic phosphorus by the dinoflagellate Prorocentrum donghaiense with the dinoflagellate Alexandrium catenella and the diatom Skeletonema costatum s.l. Hydrobiologia 754, 29–41.
Qiu, Y., Laws, E.A., Wang, L., Wang, D., Liu, X., Huang, B., 2018. The potential contributions of phytoplankton cells and zooplankton fecal pellets to POC export fluxes during a spring bloom in the East China Sea. Cont. Shelf Res. 167, 32–45.
Reuss, N., 2005. In: Sediment Pigments as Biomarkers of Environmental Change. National Environmental Research Institute, National Environmental Research Institute, Roskilde, Danmark, p. 38.
Reuss, N., Conley, D.J., 2005. Effects of sediment storage conditions on pigment analyses. Limnol. Oceanogr. Methods 3, 477–487.
Reuss, N., Conley, D., Bianchi, T., 2005. Preservation conditions and the use of sediment pigments as a tool for recent ecological reconstruction in four Northern European estuaries. Mar. Chem. 95, 283–302.
Sanchez-Cabeza, J., Ruiz-Fernández, A., 2012. 210Pb sediment radiochronology: an integrated formulation and classification of dating models. Geochim. Cosmochim. Acta 82, 183–200.
Sarthou, G., Timmermans, K.R., Blain, S., Treguer, P., 2005. Growth physiology and fate of diatoms in the ocean: a review. J. Sea Res. 53, 25–42.
Shen, F., Tang, R., Sun, X., Liu, D., 2019. Simple methods for satellite identification of algal blooms and species using 10-year time series data from the East China Sea. Remote Sens. Environ. 235, 111484.
Smayda, T.J., 1997. Harmful algal blooms: their ecophysiology and general relevance to phytoplankton blooms in the sea. Limnol. Oceanogr. 42, 1137–1153.
Smayda, T.J., 2010. Adaptations and selection of harmful and other dinoflagellate species in upwelling systems. 2. Motility and migratory behaviour. Prog. Oceanogr. 85, 71–91.
Stephens, M.P., Kadko, D.C., Smith, C.R., Latasa, M., 1997. Chlorophyll-a and pheopigments as tracers of labile organic carbon at the central equatorial Pacific seafloor. Geochim. Cosmochim. Acta 61, 4605–4619.
Strom, S.L., 1993. Production of pheopigments by marine protozoa: results of laboratory experiments analysed by HPLC. Deep-Sea Res. I Oceanogr. Res. Pap. 40, 57–80.
Tang, D., Di, B., Wei, G., Ni, I.H., Oh, I.S., Wang, S., 2006. Spatial, seasonal and species variations of harmful algal blooms in the South Yellow Sea and East China Sea. Hydrobiologia 568, 245–253.
Turner, J.T., 2015. Zooplankton fecal pellets, marine snow, phytodetritus and the ocean's biological pump. Prog. Oceanogr. 130, 205–248.
Wang, B., 2006. Cultural eutrophication in the Changjiang (Yangtze River) plume: history and perspective. Estuar. Coast. Shelf Sci. 69, 471–477.
Wang, J., Zhang, Y., Li, H., Cao, J., 2012. Competitive interaction between diatom Skeletonema costatum and dinoflagellate Prorocentrum donghaiense in laboratory culture. J. Plankton Res. 35, 367–378.
Wang, L., Huang, B., Liu, X., Xiao, W., 2015. The modification and optimizing of the CHEMTAX running in the South China Sea. Acta Oceanol. Sin. 34, 124–131.
Wang, B., Xin, M., Wei, Q., Xie, L., 2018. A historical overview of coastal eutrophication in the China Seas. Mar. Pollut. Bull. 136, 394–400.
Xiao, W., Liu, X., Irwin, A.J., Laws, E.A., Wang, L., Chen, B., Zeng, Y., Huang, B., 2018. Warming and eutrophication combine to restructure diatoms and dinoflagellates. Water Res. 128, 206–216.
Xiao, X., Agusti, S., Pan, Y., Yu, Y., Li, K., Wu, J., Duarte, C.M., 2019. Warming amplifies the frequency of harmful algal blooms with eutrophication in Chinese coastal waters. Environ.Sci.Technol. 53, 13031–13041.
Xing, L., Zhao, M., Zhang, T., Yu, M., Duan, S., Zhang, R., Huh, C.-A., Liao, W.-H., Feng, X., 2016. Ecosystem responses to anthropogenic and natural forcing over the last 100 years in the coastal areas of the East China Sea. The Holocene 26, 669–677.
Yang, D., Yin, B., Sun, J., Zhang, Y., 2013. Numerical study on the origins and the forcing mechanism of the phosphate in upwelling areas off the coast of Zhejiang province, China in summer. J. Mar. Syst. 123, 1–18.
Yang, S., Han, X., Zhang, C., Sun, B., Wang, X., Shi, X., 2014. Seasonal changes in phytoplankton biomass and dominant species in the Changjiang River Estuary and adjacent seas: general trends based on field survey data 1959–2009. J. Ocean Univ. China 13, 926–934.
Yang, D., Yin, B., Chai, F., Feng, X., Xue, H., Gao, G., Yu, F., 2018. The onshore intrusion of Kuroshio subsurface water from February to July and a mechanism for the intrusion variation. Prog. Oceanogr. 167, 97–115.
Yu, R., Zhang, Q., Kong, F., Zhou, Z., Chen, Z., Zhao, Y., Geng, H., Dai, L., Yan, T., Zhou, M., 2017. Status, impacts and long-term changes of harmful algae blooms in the sea area adjacent to the Changjiang river estuary. Oceanol. Limnol. Sin. 48, 1178–1186 (in Chinese with English abstract).
Zapata, M., Garrido, J.L., 1991. Influence of injection conditions in reversed-phase high-performance liquid chromatography of chlorophylls and carotenoids. Chromatographia 31, 589–594.
Zapata, M., Rodríguez, F., Garrido, J.L., 2000. Separation of chlorophylls and carotenoids from marine phytoplankton: a new HPLC method using a reversed phase C8 column and phridine containing mobile phases. Mar. Ecol. Prog. Ser. 195, 29–45.
Zapata, M., Fraga, S., Rodríguez, F., Garrido, J.L., 2012. Pigment-based chloroplast types in dinoflagellates. Mar. Ecol. Prog. Ser. 465, 33–52.
Zhang, J., Liu, Q., Bai, L.-L., Matsuno, T., 2018. Water mass analysis and contribution estimation using heavy rare earth elements: significance of Kuroshio intermediate water to Central East China Sea shelf water. Mar. Chem. 204, 172–180.
Zhang, J., Guo, X., Zhao, L., 2019. Tracing external sources of nutrients in the East China Sea and evaluating their contributions to primary production. Prog. Oceanogr. 176, 102122.
Zhao, J., Bianchi, T.S., Li, X., Allison, M.A., Yao, P., Yu, Z., 2012. Historical eutrophication in the Changjiang and Mississippi delta-front estuaries: stable sedimentary chloropigments as biomarkers. Cont. Shelf Res. 47, 133–144.
Zhao, Y., Yu, R.C., Kong, F.Z., Wei, C.J., Liu, Z., Geng, H.X., Dai, L., Zhou, Z.X., Zhang, Q. C., Zhou, M.J., 2019. Distribution patterns of picosized and nanosized phytoplankton assemblages in the East China Sea and the Yellow Sea: implications on the impacts of Kuroshio intrusion. J.Geophys.Res.Oceans 124, 1262–1276.
Zhou, M.-J., Shen, Z.-L., Yu, R.-C., 2008. Responses of a coastal phytoplankton community to increased nutrient input from the Changjiang (Yangtze) river. Cont. Shelf Res. 28, 1483–1489.
Zhou, Z.-X., Yu, R.-C., Zhou, M.-J., 2017a. Resolving the complex relationship between harmful algal blooms and environmental factors in the coastal waters adjacent to the Changjiang River estuary. Harmful Algae 62, 60–72.
Zhou, Z.-X., Yu, R.-C., Zhou, M.-J., 2017b. Seasonal succession of microalgal blooms from diatoms to dinoflagellates in the East China Sea: a numerical simulation study. Ecol. Model. 360, 150–162.
Zhou, Z.X., Yu, R.C., Sun, C., Feng, M., Zhou, M.J., 2019. Impacts of Changjiang River discharge and Kuroshio intrusion on the diatom and dinoflagellate blooms in the East China Sea. J.Geophys.Res.Oceans 124, 5244–5257.
Zhu, Z.-Y., Ng, W.-M., Liu, S.-M., Zhang, J., Chen, J.-C., Wu, Y., 2009. Estuarine phytoplankton dynamics and shift of limiting factors: a study in the Changjiang (Yangtze River) Estuary and adjacent area. Estuar. Coast. Shelf Sci. 84, 393–401.
Zhu, Z.-Y., Wu, Y., Zhang, J., Du, J.-Z., Zhang, G.-S., 2014. Reconstruction of anthropogenic eutrophication in the region off the Changjiang Estuary and Central Yellow Sea: from decades to centuries. Cont. Shelf Res. 72, 152–162.